Singlet Oxygen in a Cell:

Spatially-Dependent Lifetimes and Quenching

Rate Constants

Marina K. Kuimova,[a,c]* *Gokhan Yahioglu,*[a,b] *and Peter R. Ogilby*[c]*

[a] Chemistry Department, Imperial College London, Exhibition Road, SW7 2AZ, UK

[b] PhotoBiotics Ltd, 21 Wilson Street, London, EC2M 2TD, UK

[c] Center for Oxygen Microscopy and Imaging, Department of Chemistry, University of Aarhus, Århus DK-8000, Denmark

Received Date:

Emails: m.kuimova@imperial.ac.uk; progilby@chem.au.dk

Keywords: Photosensitizer, intracellular viscosity, oxygen diffusion

Abstract

Singlet molecular oxygen, $O_2(a^1\Delta_g)$, can be created in a single cell from ground state oxygen, $O_2(X^3\Sigma_g^-)$, upon focused laser irradiation of an intracellular sensitizer. This cytotoxic species can subsequently be detected by its 1270 nm phosphorescence ($a^1\Delta_g \rightarrow X^3\Sigma_g^-$) with subcellular spatial resolution. The singlet oxygen lifetime determines its diffusion distance and, hence, the intracellular volume element in which singlet-oxygen-initiated perturbation of the cell occurs. In this study, the time-resolved phosphorescence of singlet oxygen produced by the sensitizers chlorin (Chl) and 5,10,15,20-tetrakis(*N*-methyl-4-pyridyl)-21*H*,23*H*-porphine (TMPyP) was monitored. These molecules localize in different domains of a living cell. The data indicate that (*i*) the singlet oxygen lifetime and (*ii*) the rate constant for singlet oxygen quenching by added NaN_3 depend on whether Chl or TMPyP was the photosensitizer. These observations likely reflect differences in the chemical and physical constituency of a given subcellular domain (*e.g.*, spatially-dependent oxygen and NaN_3 diffusion coefficients) and, as such, are evidence that singlet oxygen responds to the inherent heterogeneity of a cell. Thus, despite a relatively long intracellular lifetime, singlet oxygen does not diffuse a great distance from its site of production. This is a consequence of an apparent intracellular viscosity that is comparatively large.

Introduction

Singlet oxygen, $O_2(a^1\Delta_g)$, is the lowest excited state of molecular oxygen.[1-3] It is well-established that singlet oxygen is an oxidizing/oxygenating agent for a wide range of organic molecules.[1,4] Production of sufficient quantities of singlet oxygen in a biological environment can perturb cellular processes, and can ultimately cause cell death via apoptosis or necrosis.[5,6] The cytotoxic effect of singlet oxygen is currently used in clinical practice in a treatment modality called Photodynamic Therapy, PDT, whereby the controlled production of singlet oxygen leads to the eradication of undesired tissue.[7] Singlet oxygen production also forms part of many natural signaling pathways and is often an important response to stress in mammalian and plant cells.[8-11]

A common and convenient way to produce singlet oxygen is photosensitization.[2] In this process, a molecule (the so-called sensitizer or, in PDT, the added drug) absorbs light to populate an excited state. Most efficient sensitizers readily produce a long-lived triplet state which transfers its energy of excitation to the ground state of molecular oxygen, $O_2(X^3\Sigma_g^-)$, in a collision-dependent process. Quenching of a sensitizer excited state by $O_2(X^3\Sigma_g^-)$ to produce $O_2(a^1\Delta_g)$ kinetically competes with sensitizer fluorescence and phosphorescence. Under most circumstances, the latter are sufficiently probable, even in the presence of oxygen, to provide a convenient optical probe of the sensitizer.

Arguably, the most unambiguous way to monitor singlet oxygen is by direct observation of its phosphorescence ($a^1\Delta_g \rightarrow X^3\Sigma_g^-$) at 1270 nm. Although this phosphorescence is weak ($\phi \sim 10^{-7}$), we have shown that it can nevertheless be detected from a single cell in both steady-state and time-resolved experiments upon irradiation of a sensitizer incorporated into the cell.[12-16] A key aspect of our work is that, using a focused laser beam, sensitizer excitation can be confined to small sub-cellular spatial domains.[15,17,18]

Using this approach, it is now possible to provide unique insight into singlet-oxygen-mediated processes that occur in a cell.

The lifetime of singlet oxygen depends significantly on the surrounding environment and also exhibits characteristically large solvent isotope effects.[2] In our work on single cells thus far, we have exploited the latter to enhance the intensity of the singlet oxygen phosphorescence signal detected. Specifically, the lifetime of singlet oxygen in D_2O is ~ 67 μs[19] whereas it is ~ 3.5 μs in H_2O,[20] and this difference is manifested in the quantum efficiency of singlet oxygen phosphorescence.[2,21] As such, we routinely work under conditions in which the intracellular H_2O has been exchanged with D_2O. Most importantly, we have demonstrated that this H_2O/D_2O exchange does not affect cell viability over the time course of our experiments.[16]

In most of our previous singlet oxygen work in cells, we used a hydrophilic cationic porphyrin as a photosensitizer: 5,10,15,20-tetrakis(*N*-methyl-4-pyridyl)-21*H*, 23*H*-porphine (TMPyP). This molecule tends to accumulate in the nucleus of cells, but an appreciable amount can still be found in the cytoplasm.[14,22,23] Time-resolved singlet oxygen phosphorescence experiments performed on D_2O-incubated, TMPyP-containing cells yield an intracellular singlet oxygen lifetime of ~ 30-40 μs, irrespective of whether the data are recorded from the cytoplasm or the nucleus.[13-16] As expected based on the known solvent isotope effect (*vide supra*), this lifetime is progressively shortened for cells with an increasing ratio of intracellular H_2O to D_2O, and extrapolates to a value of ~ 3 μs in an H_2O-containing cell.[15,16]

It is now well established that "apparent" diffusion coefficients of small molecules inside a cell can be appreciably smaller than those in a homogeneous aqueous or hydrocarbon solvent.[24] This includes the apparent diffusion coefficient of intracellular oxygen.[25-28] The data recorded point to a value for the oxygen diffusion coefficient that could be up to one

order of magnitude smaller than that in 25°C bulk water. It is important to note that, given the heterogeneity of a cell and the differences in the spatial resolution of the techniques used to quantify the translational motion of oxygen, it is appropriate to speak of an average or "apparent" value for the intracellular diffusion coefficient. The comparatively small values of intracellular diffusion coefficients are consistent with independent data that point to subcellular domains that can be quite viscous.[29]

For the present study, we set out to record singlet oxygen data that reflected the heterogeneity of a single cell. On one hand, we were interested in seeing if we could obtain spatially-dependent lifetimes of singlet oxygen that might reflect the unique chemical composition of a given domain. Thus far, direct evidence for subcellular spatially-dependent differences in singlet oxygen lifetimes has not been presented. On the other hand, we wanted to ascertain if the rate constant for the quenching of singlet oxygen by an added molecule likewise depended on the subcellular domain that was probed. For the latter study, the chemical composition of a given domain is not as important as the diffusion rate of species in that domain (*i.e.*, the viscosity of the local environment). To support this intracellular quenching study, we performed control experiments using sucrose solutions to examine the effects of a viscosity change on the quenching rate constant and, thereby, establish a reference framework for data recorded from a cell.

A key premise in our experiments is the fact that the intracellular environment is highly heterogeneous and, since the intracellular diffusion coefficient of oxygen can be small, one could create populations of singlet oxygen confined to selected subcellular domains. Although we can impart spatial resolution to our experiments by irradiating the sensitizer in the cell with a focused laser, our present beam waist (diameter ~ 1 μm)[15,18] is still large relative to the structures that define intracellular heterogeneity. As such, we chose to work

with both hydrophobic (chlorin, Chl) and hydrophilic (TMPyP) sensitizers (Figure 1), expecting that these molecules would localize in different domains of the cell.

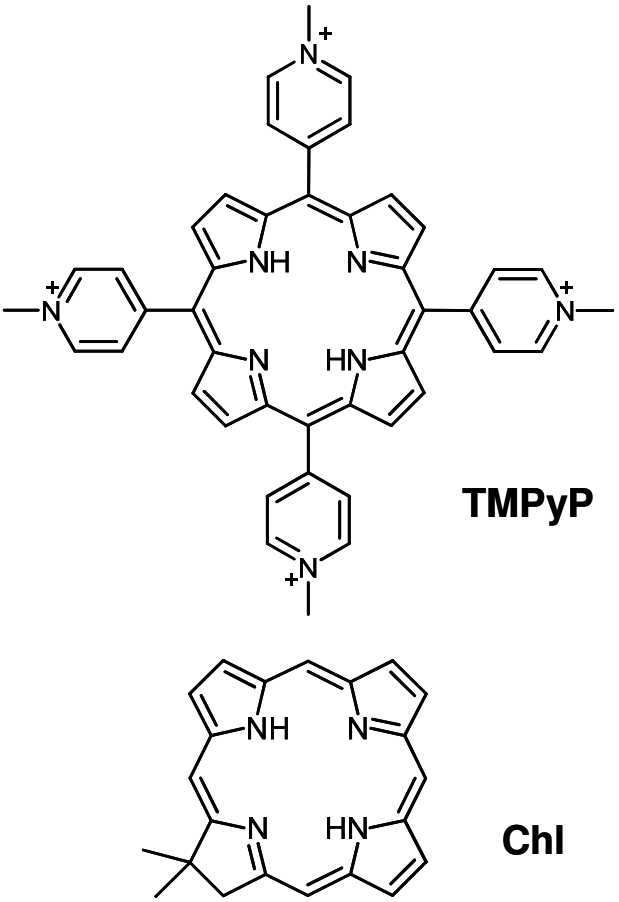

Figure 1. Structures of the photosensitizers used in this study.

Materials and Methods

Cell Preparation and Handling. HeLa cells were cultured and maintained using methods described in detail elsewhere.[16]

For experiments in which singlet oxygen phosphorescence is detected from single cells, we continue to exploit the advantage of exchanging the intracellular H_2O with D_2O which results in a larger quantum efficiency of singlet oxygen emission. Although we find it

no longer necessary to have complete exchange of the H_2O with D_2O (*i.e.*, reasonable singlet oxygen signals can now be observed from cells containing up to 50% H_2O),[15,16] it is still desirable to work with cells containing D_2O. The protocol for this H_2O/D_2O exchange is based on osmotic shock and has likewise been described previously.[16] Given that the intracellular singlet oxygen lifetimes we have measured depend linearly on the H_2O/D_2O ratio in the incubating medium and that the plots extrapolate to a lifetime that is very close to that seen in neat H_2O,[15,16] we expect homogeneous replacement of intracellular H_2O by D_2O.

Experiments were performed using cells exposed to an atmosphere of 100% oxygen, a condition that results in the most intense singlet oxygen phosphorescence signal.[15,28]

Sensitizers were incorporated into the cells by incubating the cell in a medium that contained 10 μM of the dye, as previously described.[16] For Chl, a 1 mM stock solution of the dye in DMSO was diluted to a final concentration of 10 μM in the incubation medium. The small amount of DMSO present in this case (1%) facilitated the incorporation of the hydrophobic Chl. At present, it is difficult to assess the concentration of the sensitizer when it is localized in a given sub-cellular domain.

Although sodium azide is known to be toxic to cells,[30] such toxicity was not manifested in our measurements on azide-containing cells. Specifically, the combined time over which cells were incubated with sodium azide and the data recorded never exceeded 1.0 – 1.5 h. Viability assays (annexin V apoptosis assay and trypan blue exclusion assay for necrosis) performed on our cells showed no adverse effects of sodium azide over this period of time.

5,10,15,20-Tetrakis(*N*-methyl-4-pyridyl)-21*H*, 23*H*-porphine (TMPyP), sodium azide (NaN_3), and sucrose were obtained from Sigma-Aldrich and used as received. Chlorin was synthesized as previously described.[31,32]

Instrumentation. Details of the instrumentation and approach used in this study are provided elsewhere.[13-15,18,33] Briefly, cells to be studied were contained in an atmosphere-controlled chamber that was mounted onto the translation stage of an inverted microscope. Subsequent steps of irradiation and optical monitoring varied depending on the experiment.

For all kinetics experiments, the sensitizer that had been incorporated into the cell was irradiated using the output of a femtosecond laser system that had been focused into the cell using the microscope objective. The light emitted, be it singlet oxygen phosphorescence or sensitizer phosphorescence, was collected using the microscope objective, spectrally isolated using an interference filter, and transmitted to a cooled photomultiplier tube operated in a photon counting mode. In a typical experiment, excitation energies ranged from 3 to 10 nJ/pulse at a repetition rate of 1 kHz.

Cell imaging was performed by irradiating the entire cell and its surroundings with a steady-state Xe lamp using interference filters to select the appropriate excitation wavelength. Light emitted by the sample was detected through interference filters using a CCD camera (Evolution QEi controlled by ImagePro software, Media Cybernetics) placed at the image plane of the microscope. Bright-field images were recorded using the same CCD camera, and back-lighting was achieved with a tungsten lamp provided as an accessory to Olympus IX70 inverted microscope.

Singlet oxygen quantum yields were obtained in bulk solution-phase experiments by comparing the intensity of the singlet oxygen phosphorescence recorded from the sensitizer in question to that obtained from a sensitizer standard using an approach that has been described.[34]

Results and Discussion

1. General characterization of TMPyP and Chl

TMPyP is a water-soluble photosensitizer that has a comparatively large quantum yield of singlet oxygen production, $\phi_{\Delta} = 0.77 \pm 0.04$.[35] The absorption spectrum of TMPyP, which is typical of porphyrins, is shown in Figure 2. Singlet oxygen can be produced upon irradiation into either the intense Soret band at ~ 420 nm or the weaker Q-band system over the range 500-600 nm. Also shown in Figure 2 are fluorescence spectra for TMPyP in water and in an aqueous sucrose solution. The differences in these emission spectra are consistent with what has been observed for TMPyP dissolved in water and methanol and, as examined and discussed in detail elsewhere,[36] likely reflect solvent-dependent phenomena rather than aggregation. Most importantly, the singlet oxygen kinetic data that we record, see Section 2, do not depend on phenomena that influence these emission spectra.

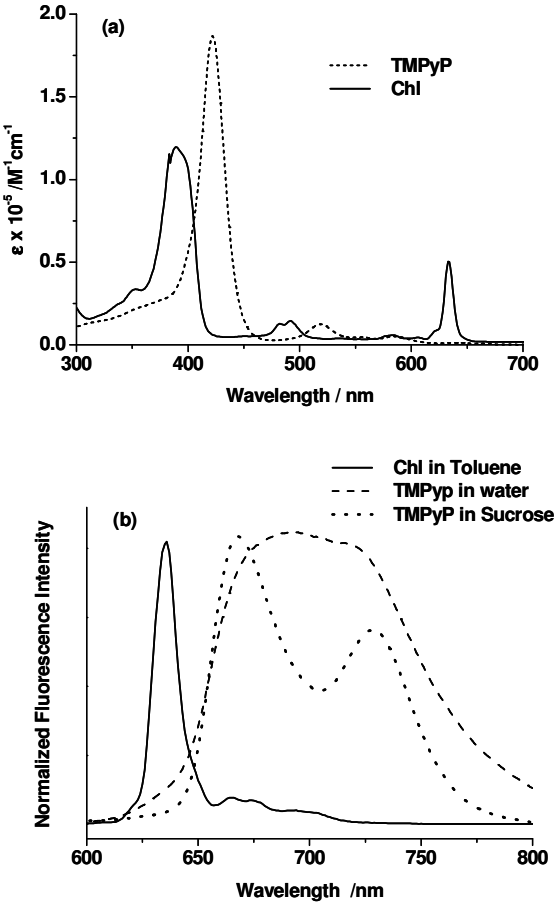

Figure 2. Absorption (a) and fluorescence (b) spectra of TMPyP in H_2O and Chl in toluene. Also shown is the fluorescence spectrum of TMPyP recorded in 1 M aqueous sucrose solution.

TMPyP is readily incorporated into a cell upon incubation of the cell in a medium that contains TMPyP.[16] Upon initial incorporation, TMPyP is first localized in lysosomes.[37,38] However, the dye eventually localizes in the nucleus (Figure 3a).[22,39] Under our cell handling conditions, experiments were invariably initiated with an intracellular TMPyP distribution such as that shown in Figure 3a.

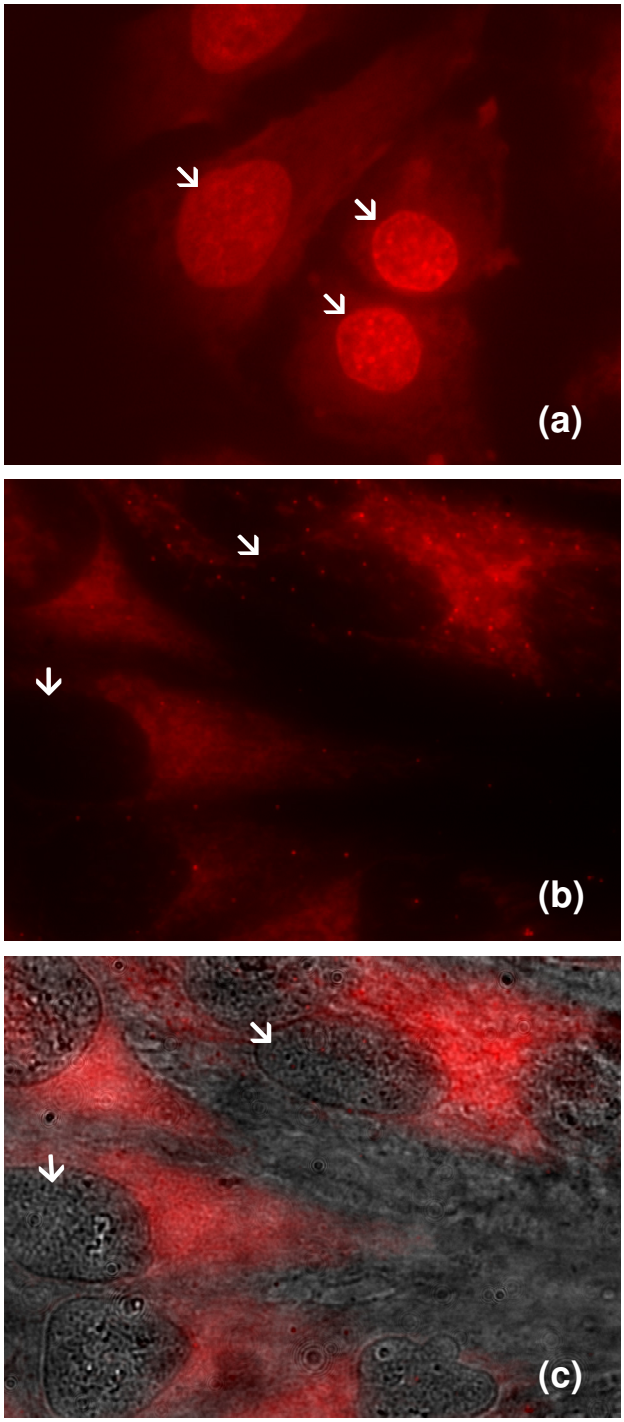

Figure 3. (a) Image of HeLa cells based on the fluorescence of TMPyP that shows the preference for this sensitizer to localize principally in the nucleus (white arrows). (b) Image of HeLa cells based on the fluorescence of Chl that shows the preference for this sensitizer to localize in the cytoplasm. Dark spots (white arrows) are the nuclei. (c) Overlay of the Chl fluorescence image shown in panel b with a transmission image that better shows the position of the nuclei (white arrows). Each image shows an area of 90 μm × 65 μm.

Chlorins are a class of porphyrin-like compounds containing one pyrrole ring that is reduced at the β-position. For our present study, we opted to use the parent, unsubstituted chlorin, Chl, which is lipophilic (Figure 1). The absorption spectrum of this compound (Figure 2) shows the characteristic features that, in general, distinguish chlorins from porphyrins.[40] We have determined that the singlet oxygen quantum yield of Chl is $\phi_\Delta = 0.44 \pm 0.05$ in toluene (obtained by monitoring the intensity of singlet oxygen phosphorescence using porphine as the standard sensitizer, $\phi_\Delta = 0.67 \pm 0.06$).[41]

Upon incorporation into a cell, Chl clearly localizes outside the nucleus in the cell cytoplasm with a distribution that appears to be quite inhomogeneous (Figure 3b). At present, we cannot determine the exact organelles and/or structures in the cytoplasm with which this hydrophobic dye associates. Nevertheless, and most importantly, the intracellular distribution of Chl is strikingly different from that of TMPyP.

2. Singlet oxygen quenching by sodium azide in sucrose solutions of different viscosity

As discussed in the Introduction, there is considerable evidence to indicate that subcellular domains can be quite viscous. With this in mind, and prior to discussing data recorded from single cells, we present results obtained from bulk aqueous solutions of sucrose. By changing the concentration of sucrose in water, one obtains solutions in which viscosity and oxygen solubility can be varied over a large range.[42,43] More importantly, these sucrose-concentration-dependent changes in viscosity and oxygen solubility have been well-quantified.[42,43] As such, singlet oxygen quenching experiments performed in sucrose solutions can be used to establish a reference framework for data recorded from a cell.

The molecule we have chosen as a singlet oxygen quencher for these studies is sodium azide, NaN_3, which readily penetrates cell membranes.[30] It is well established that NaN_3 is a

good quencher of singlet oxygen. Quenching rate constants, k_q, over the range ~ 3-6 × 10^8 $s^{-1}M^{-1}$ have been reported for experiments performed in aqueous systems, and a value as large as 5 × 10^9 $s^{-1}M^{-1}$ has been reported for CH_3CN.[44] Although these values of k_q are slightly less than the rate constant expected for a diffusion-limited process in a solvent whose viscosity is approximately 1 mPa s (*i.e.*, k_{diff} ~ 1-3 × 10^{10} $s^{-1}M^{-1}$),[45] the quenching of singlet oxygen by NaN_3 should readily approach the diffusion-controlled limit as the viscosity of the surrounding medium is increased. Although this viscosity-dependent phenomenon is general, it has been explicitly demonstrated for the quenching of singlet oxygen in a number of polymer-based systems.[46-48] We now quantify the phenomenon in aqueous liquid-phase systems suitable for comparison to data recorded from cells.

We monitor the viscosity-dependent rate of singlet oxygen quenching by NaN_3 using the time-resolved 1270 nm phosphorescence of singlet oxygen as an experimental probe. For the triplet state photosensitized production of singlet oxygen, the evolution of the phosphorescence signal, *P*, in time should follow Eq. 1.[15,20,49,50]

$$P(t) = \frac{K}{k_{rem} - k_T}\left(e^{-k_T t} - e^{-k_{rem} t}\right) \qquad (1)$$

where *K* is a scaling parameter that includes the efficiency of singlet oxygen production, k_T is the rate constant for all channels of sensitizer triplet state deactivation, and k_{rem} is the rate constant that accounts for all channels of singlet oxygen removal. In our experiments, the latter can be expressed as the sum of three terms (Eq. 2),

$$k_{rem} = k_d + k_s[S] + k_q[Q] \qquad (2)$$

where k_d is the pseudo-first-order rate constant for solvent-induced deactivation (*i.e.*, quenching by water), k_s[S] accounts for quenching by the sucrose added to change the viscosity of the solution, and k_q[Q] accounts for quenching by any other molecules (*i.e.*, in this case, added NaN_3). Note that, in aqueous and hydrocarbon systems, the rate constant for singlet oxygen radiative deactivation is small (~ 0.1 – 1.0 s^{-1})[51] compared to the rate constants for these other deactivation channels and, as such, has not been included in the expression for k_{rem}. A rate constant for singlet oxygen quenching by sucrose has been published ($k_s = 2.5 \times 10^4$ $s^{-1}M^{-1}$),[52] and we have independently confirmed this value in our present experiments (*vide infra*). Although the latter is comparatively small (*i.e.*, far removed from those in the diffusion-controlled regime), it can still be influenced by a change in viscosity.[46,47]

In systems such as ours, where $k_T \sim k_{rem}$, the observed phosphorescence signal will indeed appear as a difference of two exponential functions. In the analysis of such data, one cannot, *a priori*, assign the rising portion of the observed signal to k_T and the falling portion of the signal to k_{rem}. Rather, independent experiments and/or tests must be used to ascertain what the rate-limiting step is in the overall time evolution of the 1270 nm phosphorescence signal. This is often done in time-resolved experiments to quantify k_T (*i.e.*, sensitizer triplet absorption or phosphorescence measurements). It is also well-established that (*i*) changes in the concentration of dissolved oxygen only influence k_T, not k_{rem} (an exception occurs only in solvents where the inherent lifetime of singlet oxygen is extraordinarily long; *e.g.*, CCl_4 or CS_2), and (*ii*) changes in the H/D isotopic composition of the surrounding medium only influence k_{rem}, not k_T.[2,15] In the present study, we used both direct triplet state measurements and H/D isotopic exchange to assign the rising and decaying portions of the signal to either k_T or k_{rem}.

Time-resolved singlet oxygen phosphorescence signals were monitored as a function of NaN_3 concentration in aqueous solutions containing different amounts of sucrose. Data

recorded in solutions of 0.88 M (2.4 mPa s) and 1.96 M sucrose (19 mPa s) are shown in Figure 4. Eq. 1 was used as a fitting function for the time-resolved signals. The observed phosphorescence signals respond as expected which allows us to clearly assign values of k_T and k_{rem} to a given time-resolved trace.

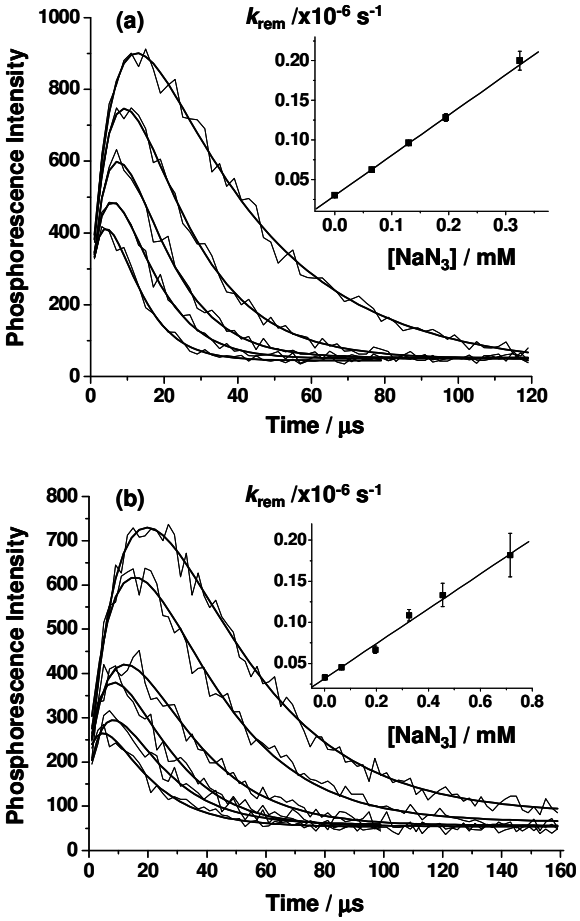

Figure 4. Time-resolved 1270 nm singlet oxygen phosphorescence traces recorded upon pulsed laser irradiation of TMPyP in air-saturated D_2O solutions containing (a) 0.88 M and (b) 1.96 M sucrose. At these sucrose concentrations, $[O_2]$ = 0.84 and 0.45 mM, respectively.[42] In each case, data were recorded with different concentrations of added NaN_3. The solid lines show fits of Eq. 1 to the data. The insets show plots of the rate constant for singlet oxygen removal, k_{rem}, against the concentration of NaN_3 (*i.e.*, Eq. 2).

With an increase in the amount of added sucrose, and the corresponding increase in viscosity and decrease in oxygen solubility,[42,43] the rate of sensitizer triplet state decay decreases reflecting a decrease in the rate of bimolecular quenching by ground state oxygen. When the values of k_{rem} obtained from the fits of Eq. 1 to the data are plotted against the sucrose concentration according to Eq. 2, we obtain a value for k_s, $(1.8 \pm 0.2) \times 10^4$ s^{-1} M^{-1}, which is consistent with published data (*vide supra*).

For all singlet oxygen phosphorescence traces recorded in a solution of the same viscosity (*i.e.*, at a given sucrose concentration), the first-order rate constant for singlet oxygen decay (k_{rem}) increases with an increase in the NaN_3 concentration, whereas the rate constant for sensitizer triplet state decay (k_T) remains constant. This is entirely consistent with the expectation that NaN_3 will not efficiently quench the sensitizer triplet state.[53] In support of this latter expectation, we independently monitored the decay rate of TMPyP phosphorescence as a function of added NaN_3 and obtained a bimolecular quenching rate constant of $(1.3 \pm 0.1) \times 10^5$ s^{-1} M^{-1} which is indeed much smaller than the rate constant for singlet oxygen quenching by NaN_3. At the limit of a highly viscous solution (*e.g.,* 1.96 M sucrose), increasing the azide concentration leads to a reversal in the magnitude of the rate constants in Eq.1 (*i.e.*, $k_{rem} > k_T$). Under these conditions, the rate of sensitizer triplet state deactivation is principally responsible for the falling part of the observed time-resolved signal, while the singlet oxygen decay is manifested on the rising part (Figure 4b).

Values of k_{rem} obtained from our fits to the time-resolved traces were plotted against the concentration of added azide (*i.e.*, Eq. 2) to yield values for the bimolecular rate constant, k_q, for singlet oxygen quenching by NaN_3 (see insets in Figure 4). The value we obtain in sucrose-free D_2O, $(5.1 \pm 0.1) \times 10^8$ s^{-1} M^{-1}, agrees well with previously published values of k_q in aqueous environments.[44]

Before discussing the viscosity dependence of singlet oxygen quenching by NaN_3, it is useful to be reminded of the general model that describes singlet oxygen quenching.[46,54] As with many other species, singlet oxygen removal can be considered to occur in two steps: (*i*) reversible diffusion in which an encounter complex is formed, and (*ii*) chemical/physical interactions within the encounter complex that result in removal (Scheme 1).

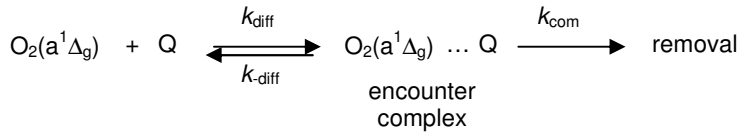

Scheme 1. General kinetic scheme used to model singlet oxygen removal by a quencher Q, where k_{diff} and k_{-diff} are the rate constants for diffusion-limited processes.

On the basis of the kinetic scheme shown, the overall quenching rate constant, k_q, that would be obtained experimentally is described by Eq. 3,[55]

$$k_q = \frac{k_{diff} k_{com}}{k_{-diff} + k_{com}} \qquad (3)$$

Two limiting conditions occur: (*i*) when $k_{com} >> k_{-diff}$, quenching will be determined by solute diffusion to form the encounter complex, and $k_q = k_{diff}$, and (*ii*) when $k_{com} << k_{-diff}$, events that occur within the encounter pair will be determining, and $k_q = (k_{diff} / k_{-diff})\, k_{com}$. The latter case defines the so-called reaction or pre-equilibrium limit.[55]

Values of k_q for the quenching of singlet oxygen by NaN_3 obtained from plots of Eq. 2 for all sucrose concentrations are plotted against the reciprocal solution viscosity in Figure 5. This plot illustrates that there are two distinct viscosity-dependent regimes in the reaction between singlet oxygen and NaN_3. At low viscosities, the rate of singlet oxygen deactivation is determined by the pre-equilibrium condition. This is consistent with the behavior of many

singlet oxygen quenchers.[47,54] As the solution viscosity is increased, however, the magnitude of the bimolecular quenching rate constant decreases indicating that the process of singlet oxygen deactivation is now determined by the rate at which singlet oxygen and NaN_3 encounter each other (*i.e.*, the diffusion-controlled limit).

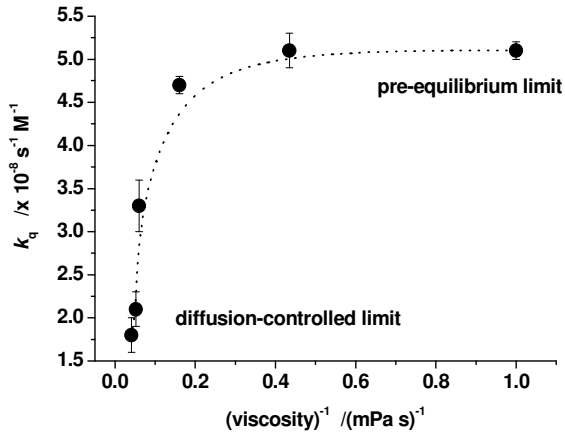

Figure 5. Rate constant for singlet oxygen quenching by NaN_3 in six different aqueous sucrose solutions plotted against the inverse viscosity of the solution.

Considering that the apparent intracellular diffusion coefficient for a small molecule such as oxygen can be comparatively small,[25-28] and that subcellular domains can have apparent viscosities that are comparatively large,[29] the data shown in Figure 5 provide the necessary framework to interpret data recorded upon the quenching of intracellular singlet oxygen by NaN_3. We note here that while the intracellular matrix is intrinsically heterogeneous, it is expected that, on a microscopic scale, homogeneous domains will exist.[29] (In this way, Figure 5 is still a pertinent reference.) The intent in our intracellular experiments is to probe the diffusion-dependent behavior of singlet oxygen kinetics in these microscopic domains.

3. Singlet oxygen production and quenching by NaN_3 in cells with TMPyP as the sensitizer

When incorporated into HeLa cells, TMPyP ultimately tends to localize in the nucleus where it most likely binds to DNA (Figure 3a).[39,56,57] Nevertheless, appreciable amounts of this hydrophilic dye appear in the cytoplasm. At present, it is unclear whether extra-nuclear TMPyP freely diffuses in the cytosol or if it binds, for example, to proteins.[58,59]

Upon irradiation of TMPyP in these respective intracellular domains, we are able to record time-resolved singlet oxygen phosphorescence signals. Note that the cross sectional diameter of the irradiating laser beam (~ 1 μm) is large relative to microscopic intracellular structures. Singlet oxygen signals recorded from the nucleus of a HeLa cell are shown in Figure 6a. The absence of a visible rising component on our signals is consistent with the high oxygen concentration used in these experiments (*i.e.*, k_T is comparatively large). Data were recorded from cells that had been exposed to a buffered medium containing concentrations of NaN_3 ranging from 0 to 0.7 mM, and clearly show a significant NaN_3-dependent increase in the rate of singlet oxygen decay. Similar data were recorded upon irradiation of TMPyP in the cytoplasm of HeLa cells.

For these intracellular experiments, the rate constant that accounts for all channels of singlet oxygen removal, k_{rem}, can be expressed as a sum of four terms (Eq. 4),

$$k_{rem} = k_d^H [H_2O] + k_d^D [D_2O] + k_c [C] + k_q [Q] \qquad (4)$$

where $k_d^H[H_2O]$ and $k_d^D[D_2O]$ are the pseudo first-order rate constants for H_2O and D_2O induced deactivation, respectively. The relative contribution of these two terms depends on the extent of H_2O/D_2O exchange in the cell. The third term, $k_c[C]$, represents all channels for singlet oxygen removal by components inherent to the cell (*e.g.*, proteins, DNA). The final term, $k_q[Q]$, accounts for quenching by added NaN_3.

The lifetimes (*i.e.*, $1/k_{rem}$) obtained in the absence of added NaN_3 are consistent with those previously reported.[13-16] Specifically, for D_2O-incubated cells, we repeatedly find that the lifetimes determined both in the cytoplasm and in the nucleus (~ 30-40 μs) are shorter than that for singlet oxygen in pure D_2O (67 μs). These data point to a non-negligible $k_c[C]$ term,[13-16] as is indeed expected given that singlet oxygen can induce cell death. The quenching plots obtained using the NaN_3-dependent lifetime data are shown in Figures 6b and 6c, and yield k_q(nucleus) = (7.8 ± 0.7) × 10^7 $s^{-1}M^{-1}$ and k_q(cytoplasm) = (1.0 ± 0.1) × 10^8 $s^{-1}M^{-1}$ for irradiation of TMPyP localized in the nucleus and cytoplasm, respectively.

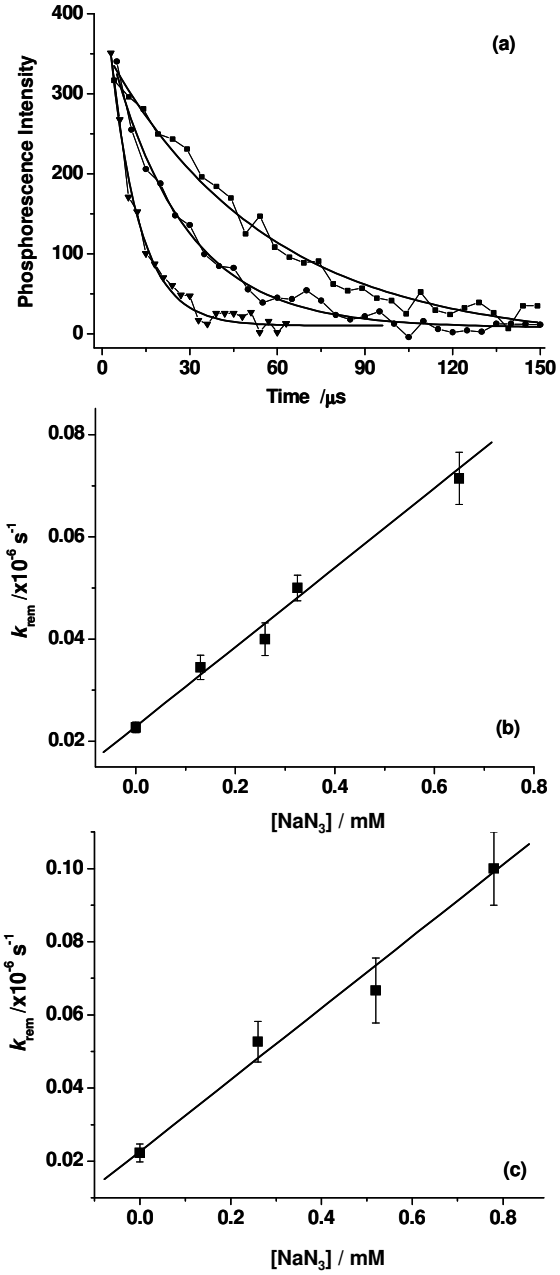

Figure 6. (a) Time-resolved singlet oxygen phosphorescence traces recorded at 1270 nm upon irradiation of TMPyP in the nucleus of oxygen-saturated HeLa cells. Data are shown for cells that had been exposed to a medium containing 0 mM (■), 0.13 mM (●), and 0.65 mM (▲) NaN_3. The lower panels show plots of the rate constant for singlet oxygen removal, k_{rem}, against the concentration of NaN_3 in the incubating medium for data recorded from the nucleus (b) and cytoplasm (c).

These rate constants for the quenching of intracellular singlet oxygen by NaN_3 are very similar to each other, and both are significantly smaller than the value obtained in neat D_2O, $k_q = 5.1 \pm 0.1 \times 10^8$ $s^{-1}M^{-1}$. Assuming that the intracellular concentration of NaN_3 equals the extracellular concentration in the incubating medium, the data in Figure 5 suggest that this intracellular quenching occurs at the diffusion-controlled limit. Moreover, in accordance with the calibration graph in Figure 5, the quenching rate constant of $(1.0 \pm 0.1) \times 10^8$ $s^{-1}M^{-1}$ corresponds to an apparent intracellular viscosity of >25 mPa s. This conclusion is further strengthened by comparison with the results of singlet oxygen quenching by NaN_3 in Chl-sensitized experiments, *vide infra*.

4. Singlet oxygen production and quenching by NaN_3 in cells with Chl as the sensitizer

As already discussed, the sensitizer Chl localizes in different intracellular domains than does TMPyP. Upon 390 nm pulsed laser irradiation of Chl in the cytoplasm, we were indeed able to observe a time-resolved emission signal at 1270 nm. However, since this is the first time Chl has been used in such an experiment, it is necessary to perform a few control experiments to ascertain that the signal we observe is indeed due to singlet oxygen phosphorescence.

First, although the phosphorescence spectrum of singlet oxygen depends slightly on solvent, the emission maximum is always ~ 1270 nm and there is no emission at 1200 nm.[60,61] Indeed, we do not observe a signal at 1200 nm, but see an appreciable signal at 1270 nm upon irradiation of intracellular Chl. Second, we observe a two-fold decrease in the intensity of our signal when the amount of oxygen in the ambient atmosphere is decreased from 100% to 60%, which is consistent with the expectation for intracellular singlet oxygen phosphorescence.[28] Third, upon successively increasing the intracellular H_2O/D_2O ratio, we see a corresponding successive increase in the decay rate of our signal (Figure 7). Although

Chl is presumably located in lipophilic domains and the singlet oxygen produced would likewise be initially located in these domains, subsequent diffusion of singlet oxygen is expected to allow for appreciable encounter with aqueous domains. As such it is not just reasonable, but indeed expected, to see a H_2O/D_2O solvent effect on such a singlet oxygen signal.[62] This point is discussed further below. Thus, in conclusion, we can assign the 1270 nm emission signal observed upon irradiation of intracellular Chl to singlet oxygen phosphorescence.

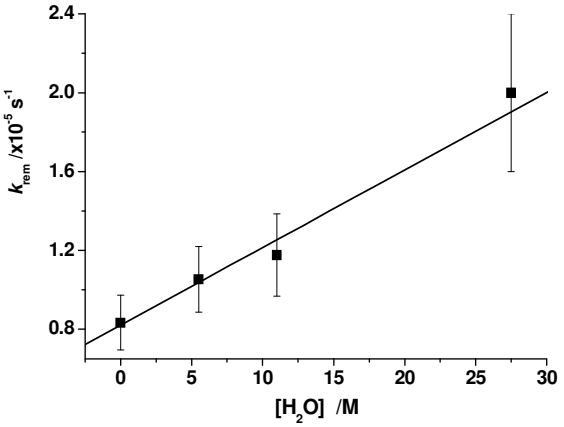

Figure 7. Plot of the rate constant for singlet oxygen removal, k_{rem}, against the concentration of H_2O in the D_2O-based medium used to incubate HeLa cells. The data were recorded upon irradiation of Chl that had been incorporated into the cells, and indicate that the intracellular lifetime in this system is indeed sensitive to the intracellular $[H_2O]/[D_2O]$ ratio.

To further characterize the Chl-sensitized intracellular singlet oxygen system, we examined the decay kinetics of the Chl triplet state which is the immediate precursor to singlet oxygen. Phosphorescence from free-base porphyrins is routinely observed with reasonable intensity over the wavelength range ~ 750-950 nm,[40] and this phosphorescence can even be observed from cells that contain an appreciable amount of oxygen.[15,50] Chl

phosphorescence can be readily detected at 800 nm from our HeLa cells (Figure 8). Upon exposing our cells to a nitrogen-saturated medium, intracellular ^{3}Chl decays with a lifetime of 8.8 ± 0.3 μs. This comparatively short lifetime can be attributed to incomplete deoxygenation of the cell. Upon exposure to an atmosphere of air, the decay rate increases yielding a lifetime of 4.8 ± 0.3 μs. Under an atmosphere of 100% oxygen, we can not differentiate between our instrument response to scattered light (τ ~ 1.5 μs) and the Chl triplet state decay. The key point here is that, under the conditions in which we observe our intracellular Chl-sensitized singlet oxygen signal (100% oxygen), we have no evidence of an intracellular population of ^{3}Chl with a lifetime longer than 4 μs. This is manifested in our singlet oxygen signals by the apparent lack of a rising component (*i.e.*, $k_T > k_{rem}$ in Eq.1.).

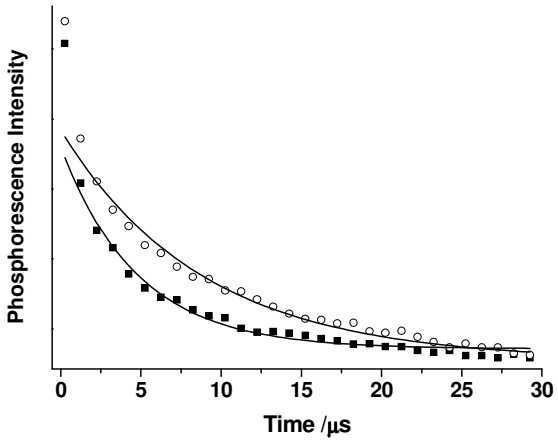

Figure 8. Time-resolved Chl phosphorescence decays recorded at 800 ± 40 nm following irradiation of Chl in a HeLa cell exposed to a nitrogen-saturated (○) and air-saturated (■) medium. The first point in each data set is in a time domain in which our signal is characterized by the system response to scattered laser light (τ ~ 1.5 μs), and these points have not been included in the exponential fits shown. Data were recorded from cells that had been incubated with a Chl-containing medium for 2 h.

After 2 h incubation of HeLa cells with a Chl-containing D_2O-based medium, we obtain a Chl-sensitized intracellular singlet oxygen lifetime of 17 ± 2 μs. It is important to note that this lifetime is appreciably shorter than those obtained when TMPyP was used as the sensitizer (*vide supra*). In itself, this is a significant observation; we are now able to provide evidence of subcellular, sensitizer-dependent singlet oxygen lifetimes. Such differences in the lifetime of intracellular singlet oxygen could reflect different chemical compositions of cellular domains (*i.e.,* different k_c[C] terms in Eq. 4). These data could also reflect partitioning of singlet oxygen between hydrophobic and hydrophilic domains (*e.g.*, one must also consider a hydrocarbon-derived solvent-dependent deactivation term in Eq. 4, k_d^{Hyd}[Hyd]). In any case, this difference in lifetimes indicates that the environment of singlet oxygen produced by either TMPyP or Chl is unique to each photosensitizer.

The Chl-sensitized intracellular singlet oxygen data are also characterized by another unique feature; the decay kinetics of the singlet oxygen phosphorescence signal depend on the elapsed time with which the HeLa cells were incubated with the medium containing Chl (Figure 9). Specifically, we observe a marked decrease in the intracellular singlet oxygen lifetime as the incubation time with the Chl-containing medium is increased. After an incubation period of 24 h, we obtain a lifetime of 4.5 ± 0.5 μs. It is reasonable to assume that this dependence on the incubation time reflects the effect of singlet oxygen quenching by the sensitizer and that, with an increased incubation period, the intracellular concentration of the sensitizer correspondingly increases (*i.e.*, we must consider yet another term in Eq. 4, k_{sens}[sens]). We have indeed substantiated this latter point by ascertaining that the distribution pattern of the intracellular Chl fluorescence does not change with an increase in the incubation time, while the intensity of the intracellular fluorescence of Chl increases markedly with incubation time.

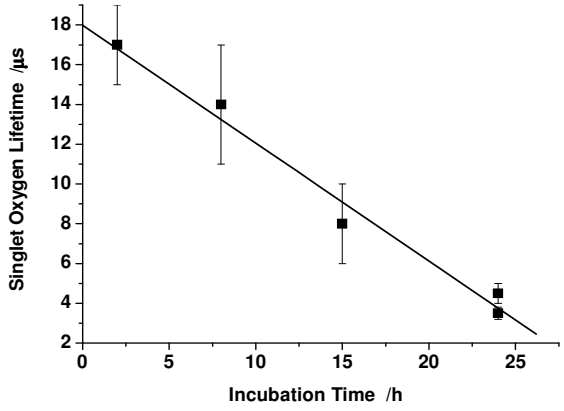

Figure 9. The singlet oxygen lifetime recorded upon irradiation of Chl incorporated in a HeLa cell as a function of the incubation time of the cell in a Chl-containing medium. The plot yields a limiting value for the lifetime of 18 ± 1 µs at an incubation time of 0 h.

In an independent control experiment, we monitored the singlet oxygen lifetime in a bulk methanol solution as a function of the Chl concentration. We likewise find that the measured lifetime decreases with an increase in the Chl concentration. From these methanol data, we obtain a rate constant of $(9 \pm 2) \times 10^8$ $s^{-1}M^{-1}$ for the quenching of singlet oxygen by Chl at the limit of low Chl concentrations ($< 2 \times 10^{-5}$ M). This number is consistent with those reported for the quenching of singlet oxygen by other porphyrin-based systems.[44] If we assume that the magnitude of this rate constant does not change appreciably with solvent, then we can use it to estimate that an intracellular Chl concentration of ~ 0.2 mM would lead to the observed change in the singlet oxygen lifetime from 17 ± 2 µs to 4.5 ± 0.5 µs.

Time-resolved singlet oxygen phosphorescence signals were recorded from Chl-containing HeLa cells as a function of the NaN_3 concentration in the incubating medium to which the cells had been exposed (Figure 10). These data were recorded using a 2 h incubation period for Chl incorporation. The quenching plot obtained using the NaN_3-dependent lifetimes (*i.e.*, Eq. 4) is shown in Figure 10b, and yields $k_q = (8 \pm 1) \times 10^8$ $s^{-1}M^{-1}$.

This value is significantly larger than those obtained in the TMPyP photosensitized experiments (*e.g.*, k_q(cytoplasm) = (1.0 ± 0.1) × 10^8 $s^{-1}M^{-1}$). Moreover, the quenching constant obtained in this Chl-photosensitised experiment is slightly larger than the value of k_q = (5.1 ± 0.1) × 10^8 $s^{-1}M^{-1}$ determined in a bulk D_2O solution (*vide supra*).

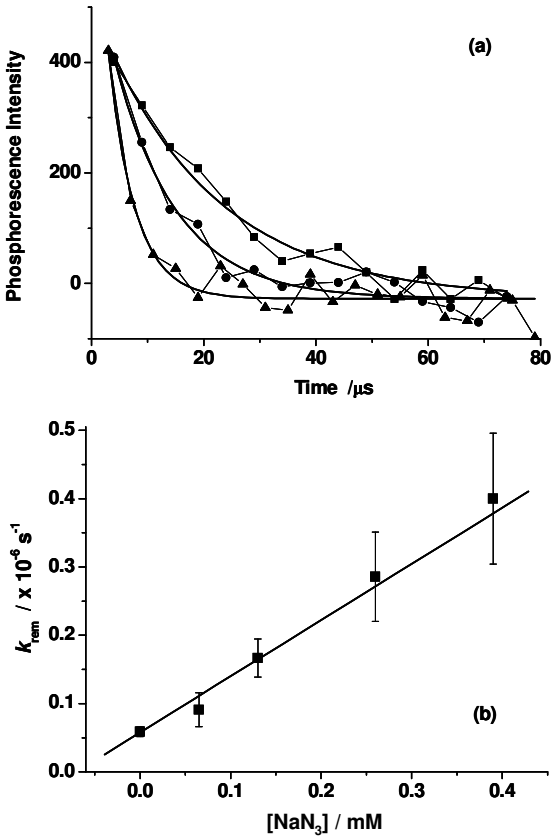

Figure 10. (a) Time-resolved singlet oxygen phosphorescence traces recorded at 1270 nm following irradiation of Chl in oxygen-saturated HeLa cells. Data are shown for cells that had been exposed to a medium containing 0 mM (■), 0.065 mM (●), and 0.26 mM (▲) NaN_3. (b) Plot of the rate constant for singlet oxygen removal, k_{rem}, obtained from traces such as those shown above against the concentration of NaN_3 in the incubating medium. The data yield a rate constant for the quenching of singlet oxygen by NaN_3 of (8 ± 1) × 10^8 s^{-1} M^{-1}.

Explanations for the differences in the magnitudes of these NaN_3 quenching rate constants must start with the recognition that, with hydrophobic Chl and hydrophilic TMPyP, singlet oxygen is produced and presumably principally localized in different domains of the heterogeneous cellular matrix. This is consistent with our lifetime data (*vide supra*). Thus, it is reasonable to suggest that the average environments seen by singlet oxygen in these respective cases are different. On this basis, a very simplistic explanation for the NaN_3 quenching rate constant in the Chl-sensitized experiment is that, in this case, an appreciable fraction of the singlet oxygen produced exists in a non-aqueous environment and the difference between k_q(Chl) in a cell and k_q(bulk D_2O) would then reflect a solvent effect on k_q. For example, compare k_q for the reaction of singlet oxygen with NaN_3 in an aqueous environment (*ca* 4×10^8 $s^{-1}M^{-1}$) and in CH_3CN (5×10^9 $s^{-1}M^{-1}$).[44]

A more general explanation for the NaN_3 quenching data is that there could be domain-dependent local gradients in the intracellular NaN_3 concentration. However, the validity of this interpretation still relies on the significant fact that the diffusion of singlet oxygen from one subcellular domain to another must be restricted due, principally, to a comparatively high intracellular viscosity.

Conclusions

Time-resolved singlet oxygen phosphorescence experiments were performed at the level of a single cell using sensitizers that localize in different subcellular domains. Sensitizer-dependent values for (*i*) the intracellular singlet oxygen lifetime and (*ii*) the rate constant for singlet oxygen quenching by added NaN_3 were obtained. The data are consistent with a model in which, irrespective of which sensitizer is used, singlet oxygen exists in intracellular domains that are more viscous than 25 °C water. Given its finite lifetime, and viscosity-dependent diffusion coefficients that can be small, it appears that singlet oxygen

lifetimes and diffusion rates are sensitive probes of the local environment. In short, we have demonstrated that singlet oxygen senses the inherent heterogeneity of a cell. This result has ramifications on issues that range from cell death to mechanisms of oxygen-dependent signal transmission.

Acknowledgements

Marina Kuimova thanks the EPSRC Life Sciences Interface Programme (UK) for a fellowship. We thank Brian Wett Pedersen for assistance in cell viability studies. This work was supported by the Danish National Research Foundation under a block grant for the Center for Oxygen Microscopy and Imaging.

References and Notes

(1) Foote, C. S.; Clennan, E. L. In *Active Oxygen in Chemistry*; Foote, C. S., Valentine, J. S., Greenberg, A., Liebman, J. F., Eds.; Chapman and Hall: London, 1995, pp 105-140.

(2) Schweitzer, C.; Schmidt, R. *Chem. Rev.* **2003**, *103*, 1685-1757.

(3) Paterson, M. J.; Christiansen, O.; Jensen, F.; Ogilby, P. R. *Photochem. Photobiol.* **2006**, *82*, 1136-1160.

(4) Clennan, E. L.; Pace, A. *Tetrahedron* **2005**, *61*, 6665-6691.

(5) Weishaupt, K. R.; Gomer, C. J.; Dougherty, T. J. *Cancer Res.* **1976**, *36*, 2326-2329.

(6) Redmond, R. W.; Kochevar, I. E. *Photochem. Photobiol.* **2006**, *82*, 1178-1186.

(7) Bonnett, R. *Chemical Aspects of Photodynamic Therapy*; Gordon and Breach Science Publishers: Amsterdam, 2000.

(8) Ledford, H. K.; Niyogi, K. K. *Plant Cell Environ.* **2005**, *28*, 1037-1045.

(9) Klotz, L.-O. *Biol. Chem.* **2002**, *383*, 443-456.

(10) Klebanoff, S. J. *Journal of Leukocyte Biology* **2005**, *77*, 598-625.

(11) Steinbeck, M. J.; Khan, A. U.; Karnovsky, M. J. *J. Biol. Chem.* **1992**, *267*, 13425-13433.

(12) Zebger, I.; Snyder, J. W.; Andersen, L. K.; Poulsen, L.; Gao, Z.; Lambert, J. D. C.; Kristiansen, U.; Ogilby, P. R. *Photochem. Photobiol.* **2004**, *79*, 319-322.

(13) Skovsen, E.; Snyder, J. W.; Lambert, J. D. C.; Ogilby, P. R. *J. Phys. Chem. B* **2005**, *109*, 8570-8573.

(14) Snyder, J. W.; Skovsen, E.; Lambert, J. D. C.; Ogilby, P. R. *J. Am. Chem. Soc.* **2005**, *127*, 14558-14559.

(15) Snyder, J. W.; Skovsen, E.; Lambert, J. D. C.; Poulsen, L.; Ogilby, P. R. *Phys. Chem. Chem. Phys.* **2006**, *8*, 4280-4293.

(16) Hatz, S.; Lambert, J. D. C.; Ogilby, P. R. *Photochem. Photobiol. Sci.* **2007**, *6*, 1106-1116.

(17) Snyder, J. W.; Zebger, I.; Gao, Z.; Poulsen, L.; Frederiksen, P. K.; Skovsen, E.; McIlroy, S. P.; Klinger, M.; Andersen, L. K.; Ogilby, P. R. *Acc. Chem. Res.* **2004**, *37*, 894-901.

(18) Skovsen, E.; Snyder, J. W.; Ogilby, P. R. *Photochem. Photobiol.* **2006**, *82*, 1187-1197.

(19) Ogilby, P. R.; Foote, C. S. *J. Am. Chem. Soc.* **1983**, *105*, 3423-3430.

(20) Egorov, S. Y.; Kamalov, V. F.; Koroteev, N. I.; Krasnovsky, A. A.; Toleutaev, B. N.; Zinukov, S. V. *Chem. Phys. Lett.* **1989**, *163*, 421-424.

(21) Ogilby, P. R. *Acc. Chem. Res.* **1999**, *32*, 512-519.

(22) Breitenbach, T.; Kuimova, M. K.; Gbur, P.; Hatz, S.; Schack, N. B.; Pedersen, B. W.; Lambert, J. D. C.; Poulsen, L.; Ogilby, P. R. *Photochem. Photobiol. Sci.* **2008**, *7*, DOI:10.1039/B809049A.

(23) By definition, the cytoplasm is the non-nuclear portion of a cell that contains a multitude of membrane-bound organelles suspended in the so-called cytosol.

(24) Kao, H. P.; Abney, J. R.; Verkman, A. S. *J. Cell Biology* **1993**, *120*, 175-184.

(25) Uchida, K.; Matsuyama, K.; Tanaka, K.; Doi, K. *Respiration Physiology* **1992**, *90*, 351-362.

(26) Dutta, A.; Popel, A. S. *J. Theor. Biol.* **1995**, *176*, 433-445.

(27) Sidell, B. D. *J. Expt. Biol.* **1998**, *201*, 1118-1127.

(28) Hatz, S.; Poulsen, L.; Ogilby, P. R. *Photochem. Photobiol.* **2008**, *84*, 1284-1290.

(29) Kuimova, M. K.; Yahioglu, G.; Levitt, J. A.; Suhling, K. *J. Am. Chem. Soc.* **2008**, *130*, 6672-6673.

(30) Leary, S. C.; Hill, B. C.; Lyons, C. N.; Carlson, C. G.; Michaud, D.; Kraft, C. S.; Ko, K.; Glerum, D. M.; Moyes, C. D. *J. Biol. Chem.* **2002**, *277*, 11321-11328.

(31) Laha, J. K.; Muthiah, C.; Taniguchi, M.; McDowell, B. E.; Ptaszek, M.; Lindsey, J. S. *J. Org. Chem.* **2006**, *71*, 4092-4102.

(32) Taniguchi, M.; Ptaszek, M.; McDowell, B. E.; Lindsey, J. S. *Tetrahedron* **2007**, *63*, 3840-3849.

(33) Arnbjerg, J.; Johnsen, M.; Frederiksen, P. K.; Braslavsky, S. E.; Ogilby, P. R. *J. Phys. Chem. A* **2006**, *110*, 7375-7385.

(34) Scurlock, R. D.; Nonell, S.; Braslavsky, S. E.; Ogilby, P. R. *J. Phys. Chem.* **1995**, *99*, 3521-3526.

(35) Frederiksen, P. K.; McIlroy, S. P.; Nielsen, C. B.; Nikolajsen, L.; Skovsen, E.; Jørgensen, M.; Mikkelsen, K. V.; Ogilby, P. R. *J. Am. Chem. Soc.* **2005**, *127*, 255-269.

(36) Vergeldt, F. J.; Koehorst, R. B. M.; van Hoek, A.; Schaafsma, T. J. *J. Phys. Chem.* **1995**, *99*, 4397-4405.

(37) Patito, I. A.; Rothmann, C.; Malik, Z. *Biol. Cell* **2001**, *93*, 285-291.

(38) Rück, A.; Köllner, T.; Dietrich, A.; Strauss, W.; Schneckenburger, H. *J. Photochem. Photobiol, B: Biol.* **1992**, *12*, 403-412.

(39) Snyder, J. W.; Lambert, J. D. C.; Ogilby, P. R. *Photochem. Photobiol.* **2006**, *82*, 177-184.

(40) Gouterman, M. In *The Porphyrins*; Dolphin, D., Ed.; Academic Press: New York, 1978; Vol. 3, pp 1-165.

(41) Ganzha, V. A.; Gurinovich, G. P.; Dzhagarov, B. M.; Egorova, G. D.; Sagun, E. I.; Shul'ga, A. M. *J. Appl. Spectrosc.* **1989**, *50*, 402-406.

(42) Rischbieter, E.; Schumpe, A. *J. Chem. Eng. Data* **1996**, *41*, 809-812.

(43) Mathlouthi, M.; Genotelle, J. In *Sucrose: Properties and Applications*; Mathlouthi, M., Reiser, P., Eds.; Blackie, 1995, pp 126-154.

(44) Wilkinson, F.; Helman, W. P.; Ross, A. B. *J. Phys. Chem. Ref. Data* **1995**, *24*, 663-1021.

(45) Ware, W. R. *J. Phys. Chem.* **1962**, *66*, 455-458.

(46) Ogilby, P. R.; Dillon, M. P.; Kristiansen, M.; Clough, R. L. *Macromolecules* **1992**, *25*, 3399-3405.

(47) Scurlock, R. D.; Kristiansen, M.; Ogilby, P. R.; Taylor, V. L.; Clough, R. L. *Polym. Degrad. Stab.* **1998**, *60*, 145-159.

(48) Turro, N. J.; Chow, M.-F.; Blaustein, M. A. *J. Phys. Chem.* **1981**, *85*, 3014-3018.

(49) Baier, J.; Maier, M.; Engl, R.; Landthaler, M.; Bäumler, W. *J. Phys. Chem. B* **2005**, *109*, 3041-3046.

(50) Jiménez-Banzo, A.; Sagrista, M. L.; Mora, M.; Nonell, S. *Free Rad. Biol. Med.* **2008**, *44*, 1926-1934.

(51) Poulsen, T. D.; Ogilby, P. R.; Mikkelsen, K. V. *J. Phys. Chem. A* **1998**, *102*, 9829-9832.

(52) Egorov, S. Y.; Krasnovsky, A. A. *Sov. Plant Physiol.* **1986**, *33*, 5-8.

(53) Nilsson, R.; Kearns, D. R.; Merkel, P. B. *Photochem. Photobiol.* **1972**, *16*, 109-116.

(54) Gorman, A. A.; Hamblett, I.; Lambert, C.; Spencer, B.; Standen, M. C. *J. Am. Chem. Soc.* **1988**, *110*, 8053-8059.

(55) Rice, S. A. In *Comprehensive Chemical Kinetics*; Bamford, C. H., Tipper, C. F. H., Compton, R. G., Eds.; Elsevier: New York, 1985; Vol. 25, pp 1-404.

(56) Kruk, N. N.; Dzhagarov, B. M.; Galievsky, V. A.; Chirvony, V. S.; Turpin, P.-Y. *J. Photochem. Photobiol., B: Biology* **1998**, *42*, 181-190.

(57) Borissevitch, I. E.; Gandini, S. *J. Photochem. Photobiol, B., Biol.* **1998**, *43*, 112-120.

(58) Borissevitch, I. E.; Tominaga, T. T.; Schmitt, C. C. *J. Photochem. Photobiol, A: Chem.* **1998**, *114*, 201-207.

(59) Lang, K.; Mosinger, J.; Wagnerova, D. M. *Coord. Chem. Rev.* **2004**, *248*, 321-350.

(60) Macpherson, A. N.; Truscott, T. G.; Turner, P. H. *J. Chem. Soc. Faraday Trans.* **1994**, *90*, 1065-1072.

(61) Wessels, J. M.; Rodgers, M. A. J. *J. Phys. Chem.* **1995**, *99*, 17586-17592.

(62) Ehrenberg, B.; Anderson, J. L.; Foote, C. S. *Photochem. Photobiol.* **1998**, *68*, 135-140.